

# Collective Behavior of Asperities in Dry Friction at Small Velocities

František Slanina

*Institute of Physics, Academy of Sciences of the Czech Republic Na Slovance 2, CZ-18040 Praha, Czech Republic  
and Center for Theoretical Study Jilská 1, CZ-11000 Praha, Czech Republic*

*e-mail: slanina@fzu.cz*

(October 12, 2018)

We investigate a simple model of dry friction based on extremal dynamics of asperities. At small velocities, correlations develop between the asperities, whose range becomes infinite in the limit of infinitely slow driving, where the system is self-organized critical. This collective phenomenon leads to effective aging of the asperities and results in velocity dependence of the friction force in the form  $F \sim 1 - \exp(-1/v)$ .

PACS number(s): 46.30.Pa; 64.60.Lx

## I. INTRODUCTION

Phenomena connected with mechanical properties of complex systems are subject of intensive study in the last decade. Generally speaking, the difficulty stems from the fact that both macroscopic scale and mesoscopic scale are important. For example, the contact area of two grains of sand is a mesoscopic object, but its properties result in macroscopic behavior of a sand heap. Among the whole family of such problems, the dry friction emerged in recent years as a hot subject. Besides the intrinsic interest in dynamics of contact interfaces sliding on top of each other, there are various systems studied recently, in which friction forces are dominant interactions determining the behavior. As examples, we may note two notoriously known phenomena: sand heaps and earthquakes. Equilibrium stress distribution in heaps of granular materials exhibits complicated localized structures [1,2]. Dynamics of tectonic plates gives rise to power-law distribution of earthquakes, formulated in Gutenberg-Richter law [3,4]. A one-dimensional counterpart of friction is *e. g.* the dislocation movement, which is responsible for the plasticity of metals.

At least three regimes of friction may be distinguished. First, dry friction corresponds to tangential force acting on the contact of two macroscopic solid bodies. The slot between the bodies is empty. The friction emerges as a result of the rheological properties of the sliding bodies both at the macroscopic and mesoscopic scale. Second case, the lubricated friction, differs in the fact, that the slot between bodies is filled with a liquid and the mechanical properties of mesoscopic portions of the lubricant are responsible for friction. Third, friction of a single microscopic tip on a surface may be measured, which explores the microscopic properties of the surface [5]. Here we concentrate on the first possibility, dry friction.

Dry friction is intensively studied today, both experimentally and theoretically [6,7]. The commonly accepted

picture of friction is based on the dynamics of a system of mesoscopic contacts, called asperities, scattered on the surface of the sliding bodies [8–12]. The typical size of asperities is constant, while their number is proportional to normal load. Hence the Amontons-Coulomb law, stating that the apparent contact area of two macroscopic bodies does not matter.

However, many features are not well understood, *e. g.* the velocity dependence of the friction force. It is explained either as a consequence of the plasticity of the asperities, which is considered as a thermally activated process [6] (this phenomenon is called aging of the asperities) or purely geometrically, based on self-affine shape of the surfaces [10]. Within the approach based on plasticity, logarithmic dependence of the age of the asperity on time is supposed on the basis of experimental data, which suggest logarithmic velocity dependence of the friction force. On the other hand, geometrical approach gives friction force proportional to  $v^{-1}$  for large velocities, while the behavior for small velocities depends on the fractal geometry of the surface.

In the description of the process of friction two levels may be distinguished. On the global level, the averaged effect of asperities can be successfully described using the elasto-plastic model developed by Caroli, Nozières and Velický [8,9]. This approach is effectively a single-site one. Only one asperity is changing its state and effect of all other asperities is described by effective surrounding medium. The scheme resembles remotely the coherent potential approximation (CPA) for electronic structure of alloys. The spatio-temporal correlations are considered to be of very short range, and the mutually sliding surfaces behave in uniform way.

On the other hand, the local, short time level of description must take into account processes which happen at several (or many) asperities simultaneously, or within a very short period of time, so that they cannot be considered as uncorrelated. Several approaches in this direction were already proposed, based on geometrical considerations [10,11], on Frenkel-Kontorova [13], Burridge-Knopoff and train models [14,15] or on an extremal dynamics model with elastic interactions [12].

The extremal dynamics (ED) models are very appealing, because they may grasp the “skeleton” of the problem, despite their simplicity and rudimentary nature. Generally, ED is based on the assumption that only one site is evolving during one time step, namely the site which has maximum (or minimum: it depends on the

model in question) of the dynamical variable determining the state of the system. However, the price to pay is that the time scale fixed by the frequency of the updates of single sites is not directly related to the real time measured in an experiment.

Extremal dynamics models were successfully used in modeling various systems, like invasion percolation, biological evolution [16], earthquakes [17] or dislocation movement [18,19]. The model we propose here is based on the ideas of ED models, adapted to the fact, that in friction we are interested in macroscopic movement with non-zero velocity, while most of ED models are appropriate to the case of infinitely slow movement.

Shortly, the evolution of our model proceeds at the most susceptible asperity, namely the asperity which bears maximum stress. A small mechanical perturbation, like release of stress at single site, may result in a burst of activity of large spatio-temporal extent. Following the terminology used in the theories of self-organized criticality [16], we will call such spatio-temporal areas of activity avalanches. The correlations present in the model will be described through statistical properties of the avalanches.

From time to time, the ED of asperities is interrupted by a macroscopic “slip” of the body as a whole, in which all asperities are completely renewed. By combination of ED evolution with such macroscopic slips, we introduce non-zero macroscopic sliding velocity into the model.

The rest of the article is organized as follows. In the section II the model is defined and the interpretation of the model parameters is given, in sect. III the presence of self-organized criticality is investigated for in the case of zero macroscopic velocity, while the effect of non-zero velocity on the breakdown of SOC as well as the velocity dependence of the friction force is investigated in sect. IV. The section V summarizes the results and draws conclusions from them.

## II. THE MODEL

We propose the following model. There are  $N$  point contacts, asperities, each with stress  $b$ . The quantity  $b$  will be interpreted as the elastic energy stored in the asperity. The model is one-dimensional (the generalization to realistic two-dimensional case is straightforward) with periodic boundary conditions, so the points form a closed ring. In each step, the point with highest stress  $b_{max}$  is found and released. The release of the stress means, that the point is removed. However, in order to keep the number of points constant, new point is introduced somewhere in the system.

As a zeroth approximation, the location of new point may be chosen at random. However, in reality the position of the new contact is determined by the detailed structure of the the surfaces of slide and track. The new contact is established at such place, where the surfaces are closest one to another. So, another number,  $d$  is at-

tributed to each point representing the width of the slot between the surfaces, waiting in the vicinity of the asperity for further updates (the *actual* slot directly on the asperity is zero, of course), and in the update the location of minimum  $d$  is found. Here a new asperity is reintroduced. The values of  $b$  and  $d$  of the neighbors of the old and new sites are also updated. Generally, each site has  $K - 1$  neighbors which are affected. For simplicity, we assume  $K = 2$ , and update only one neighbor (the right one).

Let us allow for very slow motion of the slider as a whole. The energy stored in the released asperity may be transferred entirely to other asperities, or a part of it may be converted into kinetic energy  $E$ . It may also happen that some of the kinetic energy is returned back to elastic energy of some asperities. It is natural to expect, that at higher velocities, the number of asperities affected by the transfer of the kinetic energy to the elastic one will be larger. We simplify this dependence by saying, that for  $E < E_{thr}$  only the nearest neighbors are affected, while for  $E \geq E_{thr}$  the slider slips macroscopically over average distance  $x_{slip}$ . The average duration of the slip is  $T_{slip}$  and after that time all parameters  $b$  and  $d$  of all asperities are newly attributed at random and  $E$  is set to 0. Then, the dynamics starts again. In this process, the kinetic energy  $\simeq E_{thr}$  the system had before the slip is dissipated. This makes a difference with the theories of one asperity dynamics, where the energy is dissipated immediately after release of a single asperity. In our model we do not describe the processes which happen during the slip, *e. g.* we do not examine the energy dissipated in course of the slip. Similarly, we do not calculate the physical velocity corresponding to the kinetic energy  $E$  during the ED evolution. So, we isolate only those contributions to the friction force and the macroscopic slider velocity, which originate in the ED process interrupted by instantaneous slips.

The average macroscopic velocity  $\Delta v$  stemming from the slips depends on the average time interval between two subsequent slips. We may determine this quantity  $\overline{\Delta t}$  in the time units of the extremal dynamics process. Its relation to physical time is not straightforward, but we suppose that this ambiguity affects only units, in which we measure time and not the general dependence of the friction force on velocity. Thus, we write simply

$$\Delta v = 1/\overline{\Delta t} \quad (1)$$

which corresponds to taking the average slip length  $x_{slip}$  as length unit and average time needed to update single asperity as a time unit. The contribution  $\Delta v$  from the ED process is dominant if the time between slips is much larger than the duration of the slip,  $\overline{\Delta t} \gg T_{slip}$  (*i. e.* slips are instantaneous events) and the real length travelled between slips during the ED dynamics  $x_{ED}$  is much shorter than the slip length,  $x_{ED} \ll x_{slip}$ .

The contribution  $\Delta F_{fri}$  to the friction force coming from this process is then proportional to the energy dis-

sipated in one slip. Because we are using arbitrary units, we identify

$$\Delta F_{\text{fri}} = E_{\text{thr}}. \quad (2)$$

Let us now describe the extremal dynamics of the model more formally. The model consists of  $N$  sites connected in ring topology. Each site  $i \in \{1, 2, \dots, N\}$  is connected to its right neighbor  $r(i)$ . The state of the model is described by the set  $(E, b_1, b_2, \dots, b_N, d_1, d_2, \dots, d_N)$  and the function  $r(i)$  which describe the connectivity of the sites. At the beginning,  $E = 0$  and both  $b_i$  and  $d_i$  are uniformly distributed in the interval  $(0,1)$ . The updating steps are the following.

(i) Find maximum stress  $b_{\text{max}} = \max_i(b_i)$  located at site  $i_{\text{max}}$ . Remember its old right neighbor  $i_{\text{old}} = r(i_{\text{max}})$ .

(ii) Find minimum slot  $d_{\text{min}}$  at site  $i_{\text{min}}$ .

(iii) Change of connectivity: The site  $i_{\text{max}}$  is removed by cutting its links to left and right nearest neighbors and re-inserted between  $i_{\text{min}}$  and the site next to it on the ring. It will have new right neighbor  $i_{\text{new}} = r(i_{\text{max}}) = r(i_{\text{min}})$ , and then set  $r(i_{\text{min}}) = i_{\text{max}}$ .

(iv) Kinetic effects: Set

$$E' = E + \delta \cdot b_{\text{max}}, \quad b'_{\text{max}} = (1 - \delta)b_{\text{max}}, \\ \Delta_1 = (b_M - b_{i_{\text{old}}})\theta(b_M - b_{i_{\text{old}}}), \quad \Delta_2 = (b_M - b_{i_{\text{new}}})\theta(b_M - b_{i_{\text{new}}})$$

If  $E' > \Delta_1 + \Delta_2$ , we set

$$E = E' - \Delta_1 - \Delta_2, \quad b'_{i_{\text{old}}} = b_{i_{\text{old}}} + \Delta_1, \quad b'_{i_{\text{new}}} = b_{i_{\text{new}}} + \Delta_2.$$

if not, we set

$$E = 0, \quad b'_{i_{\text{old}}} = b_{i_{\text{old}}} + E'/2, \quad b'_{i_{\text{new}}} = b_{i_{\text{new}}} + E'/2.$$

(v) Stress redistribution: For  $r_1, r_2$  random numbers distributed uniformly in the triangle  $0 < r_1 < r_2 < 1$  we set

$$b_{i_{\text{max}}} = r_1 b'_{\text{max}}, \quad b_{i_{\text{old}}} = b'_{i_{\text{old}}} + (r_2 - r_1)b'_{\text{max}}, \quad b_{i_{\text{new}}} = b'_{i_{\text{new}}} + (1 - r_2)b'_{\text{max}}.$$

(vi) New values of slots  $d$  are attributed to old and new neighbors as well as to site  $i_{\text{max}}$ , taking random numbers uniformly distributed in the interval  $(0,1)$ .

(vii) If  $E \geq E_{\text{thr}}$ , slip occurs, which means that  $E$  is set to 0 and  $b_i$  and  $d_i$  distributed uniformly in the interval  $(0,1)$ .

The kinetic effects and the slip involve several parameters. First, the parameter  $\delta$  describes how much of the elastic energy tends to be converted into the kinetic energy. This parameter can be interpreted as a measure of the spatial density of asperities: in the elementary process of freeing a particular asperity, more elastic energy may be converted into the kinetic one, if the density of asperities is lower. If  $\delta = 0$ , the kinetic effects are turned off.

The parameter  $b_M$  is the limit, up to which an asperity can absorb a portion of kinetic energy and convert it back to elastic energy. It should be the property of the surface itself, without any resort to the load and velocity of the slider. If  $\delta = 0$ , the parameter  $b_M$  does not enter the model.

The slip is determined by the parameter  $E_{\text{thr}}$ . In more realistic description, it would be necessary to introduce the function  $R(E)$  which would count the number of sites, including the extremal site  $i_{\text{max}}$ , which are to be updated, provided the kinetic energy has the value  $E$ . Here we take the simplest form  $R(E) = 3 + (N - 3)\theta(E - E_{\text{thr}})$ . Even this parameter should be the property of the surface, irrespectively of the load and velocity.

Finally, we comment on the interpretation of the quantity  $N$ , the average number of asperities. We suppose that it may serve as a measure of the external load. While  $N$  does not depend on the apparent contact area of the slider and the track, the asperity density, which is hidden in the parameter  $\delta$ , does.

So, in order to conform with the Amontons-Coulomb law, we expect that the surface properties will enter the velocity dependence of the friction force through the parameter  $b_M$  and combinations  $E_{\text{thr}}/N$  and  $\delta/N$ . We will see later that it is exactly the case.

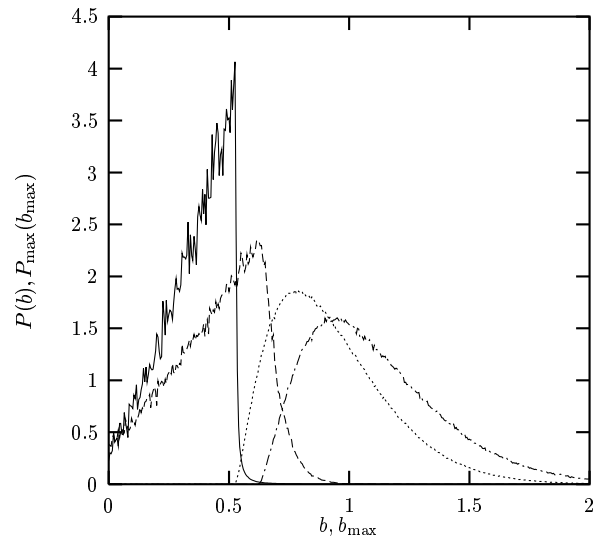


FIG. 1. Distribution of stresses  $P(b)$  and maximum stresses  $P_{\text{max}}(b_{\text{max}})$  for  $N = 1000$ ,  $\delta = 0.01$ ,  $b_M = 0.9$ . The energy threshold is infinite (full line for  $P(b)$  and dotted for  $P_{\text{max}}(b_{\text{max}})$ ) and  $E_{\text{thr}} = 0.08$  (dashed line for  $P(b)$  and dash-dotted for  $P_{\text{max}}(b_{\text{max}})$ ). Number of steps is  $10^6$ .

### III. INFINITELY SLOW MOVEMENT REGIME

Let us first investigate the case in which no slips are allowed, which can be expressed by limit value  $E_{\text{thr}} = \infty$ . In this case, the macroscopic movement is infinitely slow. If the elastic energy could not be transformed into kinetic energy  $E$ , *i. e.* if  $\delta = 0$ , the model would be a slightly more complicated version of the Zaitsev model for dislocation movement [18], which is known to be self-organized critical. The criticality manifested by power-law distribution of avalanche sizes is due to infinitely slow

driving. It is natural to expect SOC also in our model for  $\delta = 0$ . However, even for  $\delta > 0$  the condition of infinitely slow driving, which means technically that only one asperity is updated at a time, is also satisfied and SOC is expected as well.

We simulated systems of size  $N = 1000$ . The first quantity we measured was the probability distribution of the stresses,  $P(b)$  and maximum stresses  $P_{\max}(b_{\max})$ . The function  $P(b)$  is continuous up to a critical value  $b = b_c$  and then suddenly drops to zero, which is behavior common in SOC extremal dynamics models. The value of  $b_c$  depends on  $\delta$ . The typical behavior is shown in Fig. 1 for  $\delta = 0.01$ .

A fingerprint of self-organized criticality is *e. g.* the scaling behavior of the forward  $\lambda$ -avalanche sizes

$$P_{\text{fwd}}(s) = s^{-\tau} g(s|\lambda - \lambda_c|^{1/\sigma}) . \quad (3)$$

The  $\lambda$ -avalanche starts when  $b_{\max}$  exceeds the value  $\lambda$  and ends when  $b_{\max}$  drops below the value  $\lambda$  again. The size  $s$  of the avalanche is number of update steps from the start to the end of the avalanche. For numerical reasons it is simpler to investigate scaling of integrated distribution,  $P_{\text{fwd}}^>(s) = \int_s^\infty d\bar{s} P_{\text{fwd}}(\bar{s})$  from which the exponents  $\tau$  and  $\sigma$  can be determined.

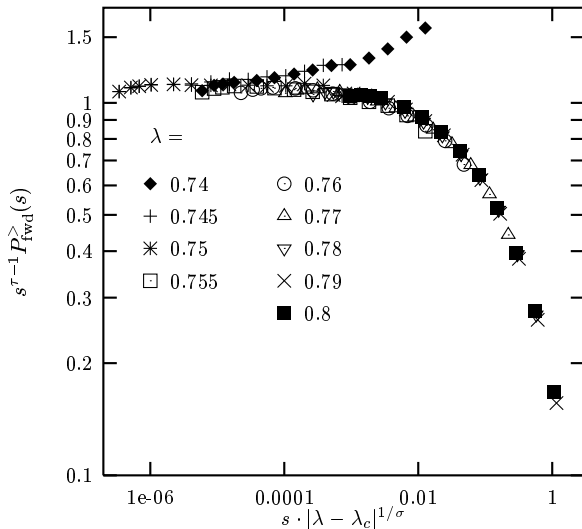


FIG. 2. Rescaled forward avalanche distribution for  $N = 1000$ ,  $\delta = 0$ . The critical threshold is  $\lambda_c = 0.7475$  and the scaling exponents  $\tau = 1.28$  and  $1/\sigma = 2.6$ . Number of steps is  $10^8$ . The corresponding thresholds  $\lambda$  are indicated next to the symbols in the legend.

The Fig. 2 and Fig. 3 show the data collapse which confirms the scaling of the form (3). Best collapse was obtained for the following values of the parameters: (a) for  $\delta = 0$  we have  $\lambda_c = 0.7475$  and  $\tau = 1.28$  and  $1/\sigma = 2.6$ . and (b) for  $\delta = 0.001$  and  $b_M = 0.9$  we have  $\lambda_c = 0.519$  and  $\tau = 1.27$ ,  $1/\sigma = 2.6$ .

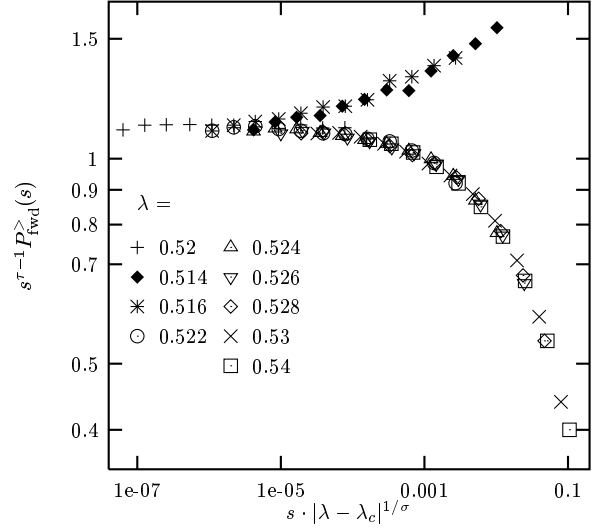


FIG. 3. Rescaled forward avalanche distribution for  $N = 1000$ ,  $\delta = 0.001$ ,  $b_M = 0.9$ . The critical threshold is  $\lambda_c = 0.519$  and the scaling exponents  $\tau = 1.27$  and  $1/\sigma = 2.6$ . Number of steps is  $10^8$ . The corresponding thresholds  $\lambda$  are indicated next to the symbols in the legend.

There is a minor difference in the exponent  $\tau$  giving best fit for  $\delta = 0$  and  $\delta = 0.001$ . However, we believe that this difference is within numerical uncertainty of the results and the model belongs to the same universality class irrespectively of parameter  $\delta$ .

By qualitative inspection of the quality of the data collapse for different choices of the exponents, we estimate the error bars. Thus, we finish with the following critical exponents of our model:

$$\tau = 1.27 \pm 0.02, \quad \sigma = 0.38 \pm 0.02 . \quad (4)$$

The forward avalanche exponent  $\tau$  is greater than in the 1D Zaitsev model [18,16], but close to the Sneppen interface growth model [20,16]. Another 1D model to be compared is the CDW model of Olami [21], and anisotropic interface depinning model of ref. [19] which have however significantly larger exponent  $\tau$ . The closest universality class seems to be the one of the Sneppen model ( $\tau = 1.26$ ), but the value of  $\sigma = 0.35$  in this class is smaller than in our model.

Whether this difference is due to finite-size effect or the two models are in different universality class cannot be stated with certainty from our present data. Instead, we would like to stress a structural similarity of the two models, which may explain the similarity of exponents. Contrary to usual interface growth models [22], the Sneppen model is a non-local one. After a single growth event (deposition of a single particle), an unbounded sequence of further steps is performed in order to re-establish the single-step property of the interface. So, the range of interactions fluctuates during the evolution, according

to the actual configuration of the interface. Similarly, the Zaitsev model, like most of other extremal dynamics models is local in the sense that after finding an extremal site, its neighbors are also updated, while the range of neighborhood is fixed. On the contrary, our model, like the Sneppen model, does not have fixed range of interactions, but it is established by the position of the minimum of the quantity  $d$  (the slot). We simulated also a version, in which the site, where new asperity is inserted, is chosen at random, instead of using the slot  $d$ . In this case we observed mean-field behavior characterized by exponents  $\tau = 1.5$ ,  $\sigma = 0.5$ .

#### IV. FRICTION AT NON-ZERO VELOCITY

In the preceding section we dealt with stationary properties of the model. In order to account for macroscopic movement, transient properties are of interest. First, we investigate the evolution of the kinetic energy  $E$  and its approach to the stationary value  $E_\infty$ , if we forbid the slips, *i. e.*  $E_{\text{thr}} = \infty$ . In Fig. 4 we show the time evolution of  $E/N$  for different values of the model parameters  $\delta$ ,  $b_M$  and number of asperities  $N$ .

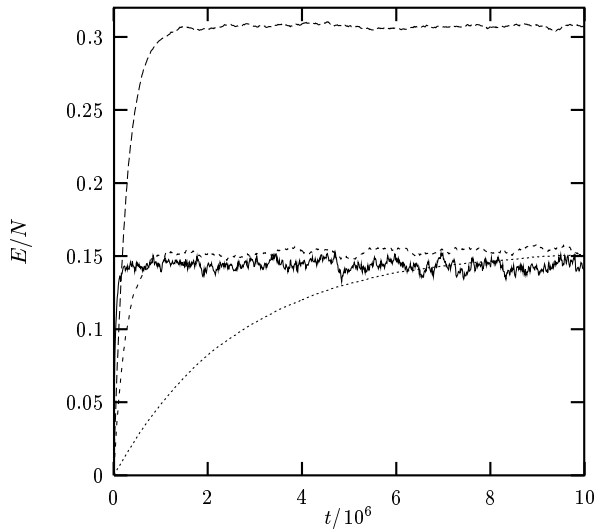


FIG. 4. Time evolution of the kinetic energy per asperity. The parameters are as follows:  $N = 1000$ ,  $\delta = 0.01$ ,  $b_M = 0.9$  (full line)  $N = 10^4$ ,  $\delta = 0.001$ ,  $b_M = 0.9$  (dotted line)  $N = 1000$ ,  $\delta = 0.001$ ,  $b_M = 0.5$  (long dashed line)  $N = 1000$ ,  $\delta = 0.001$ ,  $b_M = 0.9$  (short dashed line).

The most important observation is that the stationary value  $E_\infty/N$  depends on  $b_M$ , while the dependence on  $\delta$  and  $N$  is within the noise level. (We observe that both large  $N$  and small  $\delta$  suppress the relative fluctuations of the kinetic energy around the stationary value.) The physical significance is clear: the static friction force, which is according to eq. (2) equal to  $E_\infty$ , is proportional

to  $N$ , which is in turn proportional to normal load. Thus, we recover the Amontons-Coulomb law for static friction.

The approach of the kinetic energy to its stationary value is exponential, as is demonstrated in the Fig. 5. This type of approach is directly reflected in the velocity dependence of the friction force, as we will see below.

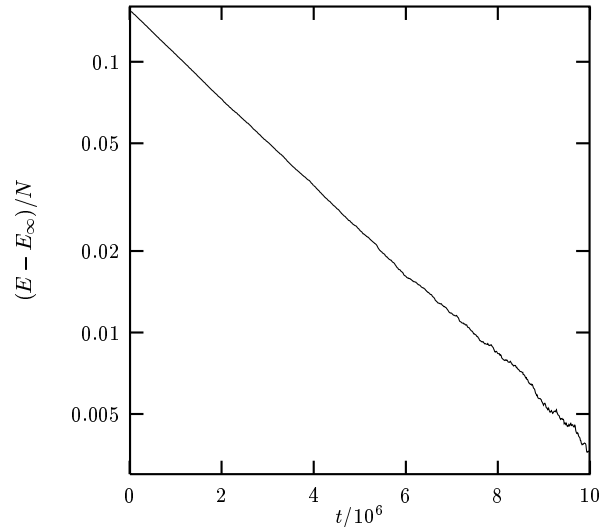


FIG. 5. Approach of the kinetic energy to its stationary value, for  $N = 10^4$ ,  $\delta = 0.001$ ,  $b_M = 0.9$ . Stationary value is taken as  $E_\infty/N = 0.155$ .

If we set the threshold  $E_{\text{thr}} < E_\infty$ , quasi-periodic behavior is observed: the kinetic energy grows, until it reaches the value of the threshold, and then the system is reinitialized. This regime is illustrated in the Fig. 6. If the threshold is close to  $E_\infty$ , the slips are less regular, due to fluctuations, but for smaller values of the threshold, the slips occur with fixed frequency. The mean number of steps  $\Delta t$  between slips is determined by the way how  $E$  approaches the stationary value. Because  $E_{\text{thr}}$  is related to the friction force by (2) and mean period of slips to the velocity, according to (1), the velocity dependence of the friction force is measurable in our model. The Fig. 7 shows the results for various  $\delta$  and  $b_M$ . If we denote  $F_0 = E_\infty$  the static friction force, we observe by plotting the velocity dependence in semi-logarithmic scale that the following law is well satisfied

$$\Delta F_{\text{fri}} = F_0 \cdot (1 - \exp(-A \frac{\delta}{\Delta v N})) \quad (5)$$

with some constant  $A$  characteristic of the model. We have found  $A = 3.6 \pm 0.3$ . The deviations from the above dependence for  $\Delta v < \delta/N$  are due to time fluctuations of  $E$ , which lead to less regular slips. However, as we already mentioned, the relative fluctuations decrease with  $N$ , so we expect the dependence (5) to hold for all velocities in thermodynamic limit  $N \rightarrow \infty$ .

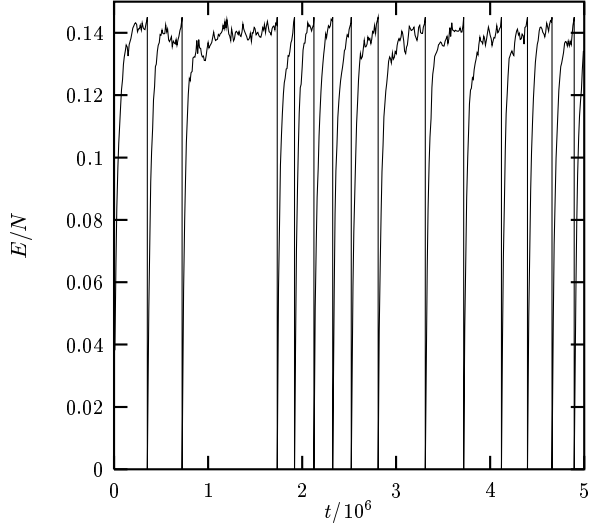


FIG. 6. Time dependence of the kinetic energy  $E$ , for  $N = 10^3$ ,  $\delta = 0.1$  and  $b_M = 0.9$ . The slips occur in the moments when  $E$  drops to 0.

As  $\delta$  is interpreted as a quantity proportional to the density of asperities, the ratio  $\delta/N$  does not depend on  $N$ , *i. e.* on the normal load. Because also  $F_0$  was found to be proportional to  $N$ , the form of (5) conforms with Amontons-Coulomb law for all  $\Delta v$ .

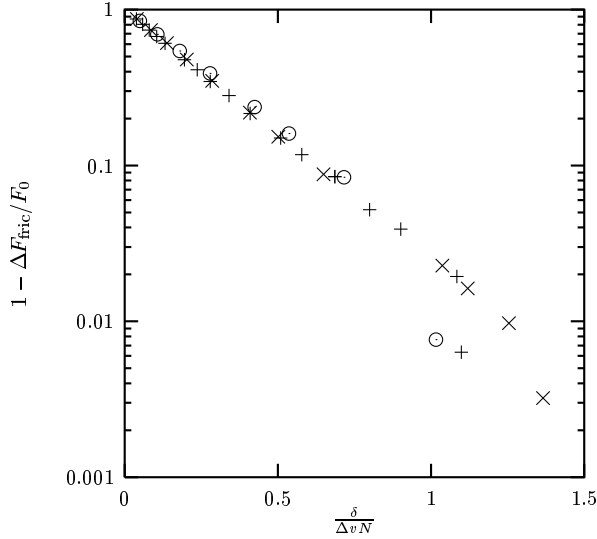


FIG. 7. Velocity dependence of the friction force, for  $N = 10^3$ ,  $\delta = 0.001$ ,  $b_M = 0.9$  (+),  $\delta = 0.001$ ,  $b_M = 0.5$  (x),  $\delta = 0.01$ ,  $b_M = 0.9$  (o).

For large velocities the friction force decreases as  $\Delta F_{\text{fri}} \sim 1/\Delta v$ . The same velocity dependence was found also using different approach [10].

Now we turn to the influence of the macroscopic move-

ment, connected to the slips on the self-organized critical behavior investigated in the last section. Each slip reinitializes the values of  $b$  and  $d$  and the evolution towards the critical attractor begins from scratch. It means that the long-range correlations characteristic for the critical state cannot fully develop. The difference can be seen already in the distribution of stresses, Fig. 1. The sharp edge in  $P(b)$  observed in the infinitely slow driving is smeared out. The position of the edge determines the critical threshold  $\lambda_c$  for the forward avalanches, so we expect that no scaling of the type (3) will hold, as soon as the macroscopic movement has non-zero velocity.

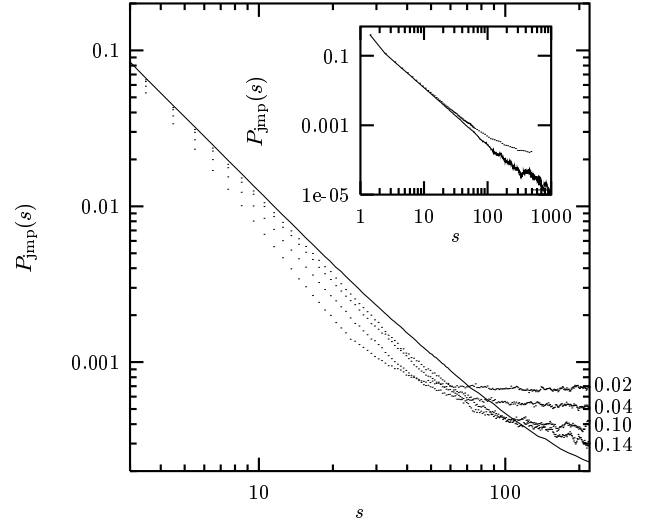


FIG. 8. Distribution of jump lengths, for  $N = 10^3$ ,  $\delta = 0.001$ ,  $b_M = 0.9$ . The full line is case without slips ( $E_{\text{thr}} = +\infty$ ). Dotted lines have slips allowed and the values of  $E_{\text{thr}}/N$  are indicated next to the position where the lines reach the right edge of the figure. In the inset, distribution of jump lengths, for  $\delta = 0$  and  $N = 10^4$  (full line) and  $N = 10^3$  (dotted line). Note that the inset makes it clear that the upward bent in the distribution for  $E_{\text{thr}} = +\infty$  is mere finite-size effect.

However, the most direct way how to investigate the breakdown of criticality due to the slips seems to us to be the calculation of the distribution of jump lengths. If in certain time step  $t$  the maximum stress was found at site  $i_t$  and in the next step at site  $i_{t+1}$ , we can compute spatial distance between this sites as follows. Let  $r_t(i)$  be the function which determines the connectivity in time  $t$ , namely  $r_t(i)$  is the site connected to  $i$  on the right-hand side. The jump length  $s$  is defined as follows: starting from  $i_t$  and applying  $r_t$  we come to the right neighbor of the extremal site at time  $t$ ,  $r_t(i_t)$ . Then, applying  $s - 1$  times the function  $r_{t+1}$  we must end at  $i_{t+1}$ . So,  $s$  is such

that  $i_{t+1} = (r_{t+1}^{\circ(s-1)} \circ r_t)(i_t)$ .

In the self-organized critical state the probability distribution of jump lengths is power law,  $P_{\text{jmp}}(s) = s^{-\pi}$ . For  $E_{\text{thr}} = \infty$  it is actually observed in our model, as indicated in the inset in the Fig. 8. The comparison of the distributions for  $N = 10^3$  and  $N = 10^4$  is shown in order to give idea of the magnitude of the finite-size corrections to the power-law behavior.

The situation with non-zero macroscopic velocity,  $E_{\text{thr}} < E_{\infty}$ , is shown in the main Fig. 8. When  $E_{\text{thr}}$  decreases, the velocity increases and the scale on which  $P_{\text{jmp}}(s)$  obeys a power law shrinks. The correlations do not have time enough to develop on the scale of the whole system, but only on shorter distances. So, we may connect the velocity dependence of the friction force to the level of correlations between the asperities, which are present in the system. Contrary to the theories where the velocity dependence stems from the aging of a single asperity, here the aging is a collective effect. The age corresponds to the range of correlations. For zero velocity the correlation length is infinite and the age is infinite as well.

## V. CONCLUSIONS

We presented a model of dry friction based on the conception of slider and track interacting through a system of asperities. We proposed an extremal dynamics model in order to describe the processes during the movement of the slider. We found the decrease of the friction force with increasing velocity. For velocities approaching to zero, the friction force has finite limit. The origin of the velocity dependence is not in a change of properties of a single asperity, but in collective effects, involving many asperities. At zero velocity, the system is in a highly correlated, self-organized critical state. The value of the exponents are close to the Sneppen interface model, however it is not clear from our data, whether the universality class is the same.

Increasing velocity gradually destroys the correlations. It is possible to view the buildup of the correlations as a collective asperity aging mechanism, as a counterpart to the single asperity aging due to plastic deformation. Such collective aging leads to different velocity dependence of the friction force than in the models considering single asperity aging and may be thus tested experimentally. Two-dimensional variant of our 1D model would be necessary for real comparison. However, the generalization to arbitrary dimension is straightforward.

This observation reveals also the limits of applicability of our model. It is appropriate in situations where the plastic deformation does not dominate. The model is applicable to the regime of very small velocities, where the usual logarithmic velocity dependence is inappropriate. It may be also used to describe friction over highly elastic surfaces, like rubber or some plastics, where the

slow aging of single asperities may not be dominant.

**Acknowledgments** I wish to thank M. Kotrla and B. Velický for useful discussions.

- 
- [1] H. M. Jaeger, S. R. Nagel and R. P. Behringer, *Physics Today* **32** (April 1996)
  - [2] F. Radjai, M. Jean, J.-J. Moreau and S. Roux, *Phys. Rev. Lett.* **77**, 274 (1996)
  - [3] P. Bak and C. Tang, *J. Geophys. Res.* **94**, 15635 (1989)
  - [4] Z. Olami, H. J. S. Feder and K. Christensen, *Phys. Rev. Lett.* **68**, 1244 (1992)
  - [5] U. D. Schwarz, O. Zwörner, P. Köster, and R. Wiesendanger, *Phys. Rev. B* **56**, 6987 (1997)
  - [6] F. Heslot, T. Baumberger, B. Perrin, B. Caroli and C. Caroli, *Phys. Rev. E* **49**, 4973 (1994)
  - [7] B. N. J. Persson and E. Tosatti, eds., *Physics of Sliding Friction*, NATO ASI Series, Applied Sciences, vol. 311, (Kluwer Academic Publishers 1996)
  - [8] C. Caroli and P. Nozières, in: *Physics of Sliding Friction*, eds. B.N.J. Persson and E. Tosatti, (Kluwer Academic Publishers, 1996) p. 27
  - [9] C. Caroli and B. Velický, *J. Phys. I France* **7**, 1391 (1997)
  - [10] A. Volmer and T. Nattermann, *cond-mat/9612206 (v2)*
  - [11] A. Tanguy and S. Roux, *Phys. Rev. E* **55**, 2166 (1997)
  - [12] A. Tanguy, M. Gounelle and S. Roux, *cond-mat/9804105*
  - [13] M. Weiss, F.-J. Elmer, *Z. Phys. B* **104**, 55 (1997)
  - [14] F.-J. Elmer, in: *Physics of Sliding Friction*, eds. B.N.J. Persson and E. Tosatti, (Kluwer Academic Publishers, 1996) p. 433
  - [15] F.-J. Elmer, *adap-org/9710002*
  - [16] M. Paczuski, S. Maslov and P. Bak, *Phys. Rev.* **53**, 414 (1996)
  - [17] K. Ito, *Phys. Rev. E* **52**, 3232 (1995)
  - [18] S. I. Zaitsev, *Physica A* **189**, 411 (1992)
  - [19] S. Maslov and Y.-C. Zhang, *Phys. Rev. Lett.* **75**, 1550 (1995)
  - [20] K. Sneppen, *Phys. Rev. Lett.* **69**, 3539 (1992)
  - [21] Z. Olami, *preprint*
  - [22] T. Halpin-Healy and Y.-C. Zhang, *Phys. Rep.* **254**, 215 (1995)